Int. J. Solids Structures Vol. 22, No. 1, pp. 87–106, 1986
Printed in Great Britain.

0020–7683/86 $3.00 + .00

SMOOTH INDENTATION OF AN ISOTROPIC CANTILEVER BEAM

LEON M. KEER and WILLIAM P. SCHONBERG
Department of Civil Engineering, Northwestern University, Evanston, IL 60201, U.S.A.

(*Received* 28 *March* 1984; *in revised form* 10 *December* 1984)

Abstract—The response of an isotropic cantilever beam of finite length under the action of frictionless cylindrical and flat indenters is studied. Solutions are obtained through a local–global technique, which accounts for both the local behavior near the indenter, as well as the global beam behavior. The method of analysis superposes an infinite-layer solution, derived through the use of integral transforms with a pure-bending beam-theory solution. Local indenter stresses, as well as displacements and rotations, are computed for each case and plotted for various ratios of contact width to beam thickness, and for various positions of the indenter. Where possible, the results are compared to Hertz theory of contact stresses and to beam-theory displacement and rotation solutions.

1. INTRODUCTION

Consider the finite layer of length l and thickness h shown in Fig. 1. The layer is fixed at one end, free on the other and loaded by an indenter centered at a distance l_0 from the fixed end. Although the theory is applicable for an arbitrary geometry, the types of indenters studied are cylindrical [Fig. 1(a)] and flat [Fig. 1(b)]. Such problems are seen quite often in mechanical applications, and may also serve as models for impact phenomena in gears and turbine blades. Usual methods, which use a beam-theory solution to obtain an overall load-displacement relationship and then a Hertzian contact solution to calculate local stresses under the indenter, are fairly limited, as will be shown in this paper. The method of solution used in this paper is the superposition of an elasticity solution with a beam-theory solution. In this way, local contact stresses are represented by the elasticity solution, while the global stresses are represented by the beam-theory solution.

A problem of the type considered here has already been solved by Keer and Miller[1], and by Keer and Ballarini[2] for a beam that is clamped or simply supported at both ends and loaded by a cylindrical indenter. Although not treated numerically here, the intermediate case of a partially fixed end can be solved for each type of indenter in a similar manner. Furthermore, the methods used in this paper can be modified and expanded to study plate or shell problems involving similar loadings[3].

The physical quantities of interest are the stress distribution under each indenter, and the displacement and rotation of the beam under each of the indenters. The ratio of contact width to beam thickness, c/h, is treated as a known parameter in both problems. In the cylindrical indenter problem, the ratio of indenter arm length to beam thickness, l_0/h, is treated as an additional known parameter. However, in the flat indenter problem, the parameter $l_1/h = l_0/h - c/h$ (i.e. the distance from the fixed end of the beam to the left-hand end of the indenter) is introduced as an additional known parameter. In this manner, for a given l_1/h, when the quantity c/h is varied over a range of values, the phenomenon known as "receding contact" can be observed in the flat indenter problem. By varying the proper parameters as required by the type of problem, then calculating deflections, rotations, loads and stresses, an extensive study of the response of an isotropic cantilever beam subjected to various loading conditions can be performed. The results obtained are compared to beam theory solutions and Hertz contact solutions for accuracy assessments.

2. CASE I: CYLINDRICAL INDENTER—PROBLEM FORMULATION

The problem to be solved is that of an elastic layer of thickness h and length l indented by a cylindrical punch on its upper surface [Fig. 1(a)]. The conditions at the

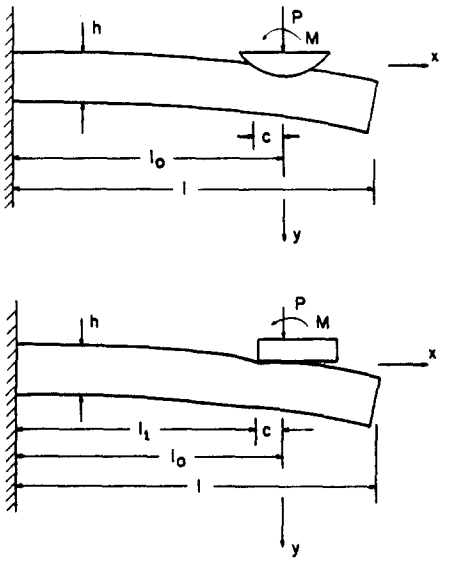

Fig. 1. (a) Problem configuration (case I). (b) Problem configuration (case II).

ends of the layer are those of a cantilever beam, clamped on the left and free on the right. The solution of the problem will be achieved by a suitable superposition and matching of an elasticity solution and a beam-theory solution.

The boundary conditions for the elasticity problem can be written as follows:

$$\tau_{yy}(x, h) = 0, \qquad |x| < \infty, \tag{2.1}$$

$$\tau_{xy}(x, h) = 0, \qquad |x| < \infty, \tag{2.2}$$

$$\tau_{xy}(x, 0) = 0, \qquad |x| < \infty, \tag{2.3}$$

$$\tau_{yy}(x, 0) = 0, \qquad c < |x| < \infty, \tag{2.4}$$

$$u_y(x, 0) = \Delta - x^2/2R, \qquad 0 < |x| < c. \tag{2.5}$$

The beam-theory boundary conditions for the ends of the layer can be written as follows:

$$\bar{\theta} = 0, \qquad x = -l_0, \tag{2.6}$$

$$u_y = 0, \qquad x = -l_0 \tag{2.7}$$

$$M = 0, \qquad x = l - l_0 \tag{2.8}$$

$$V = 0, \qquad x = l - l_0 \tag{2.9}$$

where M and V are the moment and shear, and $\bar{\theta}$ is the average value of the slope measured through the thickness given by

$$\bar{\theta} = \frac{1}{h}\int_0^h \frac{\partial u_y}{\partial x}\,dy. \tag{2.10}$$

A suitable elasticity solution that represents loading on the upper surface of an isotropic elastic layer in plane strain, and with no loading on its lower surface, is

obtained using the techniques of Sneddon[4], and is given as follows:

$$\tau_{yy} = \int_0^\infty \frac{E_S(\xi)\cos(\xi x) + E_A(\xi)\sin(\xi x)}{\beta^2 - \operatorname{sh}^2\beta} \{[\beta + \operatorname{sh}\beta \operatorname{ch}\beta + \xi y \operatorname{sh}^2\beta]\sinh(\xi y) - [\operatorname{sh}^2\beta - \beta^2 + \xi y(\beta + \operatorname{sh}\beta \operatorname{ch}\beta)]\cosh(\xi y)\}\, d\xi, \tag{2.11}$$

$$\tau_{xy} = -\int_0^\infty \frac{E_S(\xi)\sin(\xi x) - E_A(\xi)\cos(\xi x)}{\beta^2 - \operatorname{sh}^2\beta} \{[\beta^2 - \xi y(\beta + \operatorname{sh}\beta \operatorname{ch}\beta)]\sinh(\xi y) + \xi y \operatorname{sh}^2\beta \cosh(\xi y)\}\, d\xi, \tag{2.12}$$

$$\tau_{xx} = \int_0^\infty \frac{E_S(\xi)\cos(\xi x) + E_A(\xi)\sin(\xi x)}{\beta^2 - \operatorname{sh}^2\beta} \{[\beta + \operatorname{sh}\beta - \xi y \operatorname{sh}^2\beta]\sinh(\xi y) - [\beta^2 + \operatorname{sh}^2\beta - \xi y(\beta + \operatorname{sh}\beta \operatorname{ch}\beta)]\cosh(\xi y)\}\, d\xi, \tag{2.13}$$

$$2\mu u_x = \int_0^\infty \frac{E_S(\xi)\sin(\xi x) - E_A(\xi)\cos(\xi x)}{\xi(\beta^2 - \operatorname{sh}^2\beta)} \{[(1-2\nu)(\beta + \operatorname{sh}\beta \operatorname{ch}\beta) - \xi y \operatorname{sh}^2\beta]\sinh(\xi y) - [\beta^2 + (1-2\nu)\operatorname{sh}^2\beta - \xi y(\beta + \operatorname{sh}\beta \operatorname{ch}\beta)]\cosh(\xi y)\}\, d\xi, \tag{2.14}$$

$$2\mu u_y = \int_0^\infty \frac{E_S(\xi)\cos(\xi x) + E_A(\xi)\sin(\xi x)}{\xi(\beta^2 - \operatorname{sh}^2\beta)} \{[\beta^2 - 2(1-\nu)\operatorname{sh}^2\beta - \xi y(\beta + \operatorname{sh}\beta \operatorname{ch}\beta)]\sinh(\xi y) + [2(1-\nu)(\beta + \operatorname{sh}\beta \operatorname{ch}\beta) + \xi y \operatorname{sh}^2\beta]\cosh(\xi y)\}\, d\xi. \tag{2.15}$$

where $\beta = \xi h$, and μ and ν are the shear modulus and Poisson's ratio of the layer material, respectively. The corresponding equations for a layer in plane stress with the same loading conditions are obtained by replacing ν with $\nu/(1+\nu)$. Furthermore, this substitution is to be used through the rest of this paper to convert plane-strain expressions to corresponding expressions in plane stress.

It is seen that on $y = h$, the normal and shear stresses vanish automatically, and that on $y = 0$, the shear stresses vanish. The normal stress on $y = 0$ is given as

$$\tau_{yy}(x, 0) = \int_0^\infty [E_S(\xi)\cos(\xi x) + E_A(\xi)\sin(\xi x)]\, d\xi. \tag{2.16}$$

We let

$$E_S(\xi) = \int_0^c \psi(t) J_0(\xi t)\, dt, \tag{2.17}$$

$$E_A(\xi) = \int_0^c \phi(t) J_1(\xi t)\, dt. \tag{2.18}$$

Then eqn (2.16) becomes

$$\tau_{yy}(x, 0) = \int_x^c \frac{\psi(t)\, dt}{\sqrt{(t^2 - x^2)}} + x\int_x^c \frac{\phi(t)\, dt}{t\sqrt{(t^2 - x^2)}}. \tag{2.19}$$

The moment and shear, due to the stresses as given by eqns (2.11)–(2.13), are given by

$$M_E(x) = \int_0^h y\tau_{xx}\,dy = -\int_0^\infty [E_S(\xi)\cos(\xi x) + E_A(\xi)\sin(\xi x)]\frac{d\xi}{\xi^2}, \tag{2.20}$$

$$V_E(x) = \int_0^h \tau_{xy}\,dy = \int_0^\infty [E_S(\xi)\sin(\xi x) - E_A(\xi)\cos(\xi x)]\frac{d\xi}{\xi}. \tag{2.21}$$

We note that eqns (2.20) and (2.21) satisfy the condition

$$V = \frac{dM}{dx}. \tag{2.22}$$

From eqns (2.10) and (2.15), the average value of the slope is found to be given by

$$\bar{\theta}_E(x) = \frac{1}{2\mu}\int_0^\infty \frac{\beta - (3-2\nu)\,\mathrm{sh}\,\beta}{\beta(\beta - \mathrm{sh}\,\beta)}[E_S(\xi)\sin(\xi x) - E_A(\xi)\cos(\xi x)]\,d\xi. \tag{2.23}$$

For the beam theory solution, the displacement is taken to be of the form

$$u_y^B(x) = a_0 + a_1 x + a_2 x^2 + a_3 x^3. \tag{2.24}$$

Assuming the hypotheses of Euler–Bernoulli beam theory, the following results are obtained:

$$u_x^B(x) = -\frac{\partial u_y^B}{\partial x}\left(y - \frac{h}{2}\right), \tag{2.25}$$

$$\tau_{xx}^B = \frac{2\mu}{1-\nu}\frac{\partial u_x^B}{\partial x}. \tag{2.26}$$

Using eqns (2.24)–(2.26), the moment, shear and average slope are calculated to be

$$M_B(x) = \int_0^h y\tau_{xx}\,dx = -2D(a_2 + 3a_3 x), \tag{2.27}$$

$$V_B(x) = \int_0^h \tau_{xy}\,dx = -6Da_3, \tag{2.28}$$

$$\bar{\theta}_B(x) = \frac{1}{h}\int_0^h \frac{\partial u_x^B}{\partial x}\,dy = a_1 + 2a_2 x + 3a_3 x^2, \tag{2.29}$$

where $D = \mu h^3/6(1-\nu)$. Thus the solution sought will be a superposition of the elasticity solution given by eqns (2.11)–(2.16) and (2.20)–(2.23), and the beam theory solution given by eqns (2.24)–(2.29). The two solutions are matched properly when the boundary conditions, eqns (2.1)–(2.9), are all satisfied. This is achieved by solving for the constants a_1, a_2 and a_3 by superposing the two solutions and applying the beam-theory boundary conditions. Thus eqns (2.6), (2.8) and (2.9) become

$$M_E(l - l_0) + M_B(l - l_0) = 0, \tag{2.30}$$

$$V_E(l - l_0) + V_B(l - l_0) = 0, \tag{2.31}$$

$$\bar{\theta}_E(-l_0) + \bar{\theta}_B(-l_0) = 0. \tag{2.32}$$

Applying eqns (2.20)–(2.23) and (2.24)–(2.29) to eqns (2.30)–(2.32) yields the following:

$$a_1 = -\frac{1}{D}\int_0^\infty \left\{\frac{l_0(l - l_0/2)}{\xi}\left[E_S(\xi)\sin\xi(l - l_0) - E_A(\xi)\cos\xi(l - l_0)\right]\right.$$
$$\left. + \frac{l_0}{\xi^2}\left[E_S(\xi)\cos\xi(l - l_0) + E_A(\xi)\sin\xi(l - l_0)\right]\right\} d\xi$$
$$+ \frac{1}{2\mu}\int_0^\infty \frac{\beta - (3 - 2\nu)\,\mathrm{sh}\,\beta}{\beta(\beta - \mathrm{sh}\,\beta)}\left[E_S(\xi)\sin(\xi l_0) + E_A(\xi)\cos(\xi l_0)\right] d\xi, \quad (2.33)$$

$$a_2 = -\frac{1}{2D}\int_0^\infty \left[E_S(\xi)\cos\xi(l - l_0) + E_A(\xi)\sin\xi(l - l_0)\right]\frac{d\xi}{\xi^2}$$
$$- \frac{l - l_0}{2D}\int_0^\infty \left[E_S(\xi)\sin\xi(l - l_0) - E_A(\xi)\cos\xi(l - l_0)\right]\frac{d\xi}{\xi}, \quad (2.34)$$

$$a_3 = \frac{1}{6D}\int_0^\infty \left[E_S(\xi)\sin\xi(l - l_0) - E_A(\xi)\cos\xi(l - l_0)\right]\frac{d\xi}{\xi}. \quad (2.35)$$

The two remaining boundary conditions given by eqns (2.5) and (2.7) still need to be satisfied. First, consider eqn (2.5):

$$u_y^E(x, 0) + u_y^B(x, 0) = \Delta - x^2/2R. \quad (2.36)$$

Differentiating with respect to x,

$$\frac{\partial u_y^E}{\partial x}(x, 0) + \frac{\partial u_y^B}{\partial x}(x, 0) = -\frac{x}{R}. \quad (2.37)$$

Separating eqn (2.37) into a symmetric and an antisymmetric part, with respect to x, yields

$$\frac{\partial u_y^E}{\partial x}(x, 0)\bigg|_A + 2a_2x = -\frac{x}{R}, \quad (2.38)$$

$$\frac{\partial u_y^E}{\partial x}(x, 0)\bigg|_S + a_1 + 3a_3x^2 = 0. \quad (2.39)$$

Consider first eqn (2.38). Substituting for $u_y^E(x, 0)$ according to eqn (2.15), combining terms in $E_S(\xi)$ and $E_A(\xi)$, and making use of eqns (2.17) and (2.18) yields

$$\int_0^c \psi(t)\int_0^\infty \left[\frac{h^3}{6}\left(\frac{\beta + \mathrm{sh}\,\beta\,\mathrm{ch}\,\beta}{\beta^2 - \mathrm{sh}^2\,\beta}\right)\sin(\xi x) + \frac{x}{\xi^2}\cos\xi(l - l_0) + \frac{x(l - l_0)}{\xi}\right.$$
$$\left.\times \sin\xi(l - l_0)\right] J_0(\xi t)\,d\xi\,dt + \int_0^c \phi(t)\int_0^\infty \left[\frac{x}{\xi^2}\sin\xi(l - l_0)\right.$$
$$\left. - \frac{x(l - l_0)}{\xi}\cos\xi(l - l_0)\right] J_1(\xi t)\,d\xi\,dt = \frac{Dx}{R}. \quad (2.40)$$

An asymptotic evaluation of the kernels in eqn (2.40) shows that they are all convergent at the lower limit of integration. However, at the upper limit, the first term in the first kernel is divergent. This is adjusted by adding and subtracting the term

$$\frac{h^3}{6}\int_0^c \psi(t)\int_0^\infty \sin(\xi x)J_0(\xi t)\,d\xi\,dt$$

in eqn (2.40) as follows:

$$-\frac{h^3}{6}\int_0^c \psi(t)\int_0^\infty \sin(\xi x)J_0(\xi t)\,d\xi\,dt + \int_0^c\left[\frac{h^3}{6}\left(\frac{\beta + \operatorname{sh}\beta\operatorname{ch}\beta}{\beta^2 - \operatorname{sh}^2\beta} + 1\right)\sin(\xi x)\right.$$
$$\left. + \frac{x}{\xi^2}\cos\xi(l - l_0) + \frac{x(l - l_0)}{\xi}\sin\xi(l - l_0)\right]J_0(\xi t)\,d\xi\,dt$$
$$+\int_0^c \phi(t)\int_0^\infty\left[\frac{x}{\xi^2}\sin\xi(l - l_0) - \frac{x(l - l_0)}{\xi}\cos\xi(l - l_0)\right]J_1(\xi t)\,d\xi\,dt = \frac{Dx}{R}. \tag{2.41}$$

After simplification (i.e. through use of the Weber–Schafheitlin integral[5]), eqn (2.41) reduces to

$$\frac{h^3}{6}\psi(x) - \int_0^c \psi(t)K_1(x, t)\,dt - \int_0^c \phi(t)K_2(x, t)\,dt = -\frac{Dx}{R}, \tag{2.42}$$

where

$$K_1(x, t) = \int_0^\infty\left[\frac{h^3}{6}\left(\frac{\beta + \operatorname{sh}\beta\operatorname{ch}\beta}{\beta^2 - \operatorname{sh}^2\beta} + 1\right)\xi x J_0(\xi x)\right.$$
$$\left. + \frac{x}{\xi^2}\cos\xi(l - l_0)\right]J_0(\xi t)\,d\xi + \frac{\pi}{2}x(l - l_0), \tag{2.43}$$
$$K_2(x, t) = \frac{\pi}{4}tx. \tag{2.44}$$

Returning to eqn (2.39), performing similar manipulations yields

$$\int_0^c \phi(t)\int_0^\infty\left\{\frac{h^3}{6}\frac{\beta + \operatorname{sh}\beta\operatorname{ch}\beta}{\beta^2 - \operatorname{sh}^2\beta}\cos(\xi x) + \frac{h^3}{12(1 - \nu)}\frac{\beta - (3 - 2\nu)\operatorname{sh}\beta}{\beta(\beta - \operatorname{sh}\beta)}\cos(\xi l_0)\right.$$
$$\left. + \frac{l_0(l - l_0/2)}{\xi}\cos\xi(l - l_0) - \frac{l_0}{\xi^2}\sin\xi(l - l_0) - \frac{x^2}{2\xi}\cos\xi(l - l_0)\right\}J_1(\xi t)\,d\xi\,dt$$
$$+\int_0^c \psi(t)\int_0^\infty\left\{\frac{h^3}{12(1 - \nu)}\frac{\beta - (3 - 2\nu)\operatorname{sh}\beta}{\beta(\beta - \operatorname{sh}\beta)}\sin(\xi l_0) - \frac{l_0(l - l_0/2)}{\xi}\sin\xi(l - l_0)\right.$$
$$\left. + \frac{x^2}{2\xi}\sin\xi(l - l_0) - \frac{l_0}{\xi^2}\cos\xi(l - l_0)\right\}J_0(\xi t)\,d\xi\,dt = 0. \tag{2.45}$$

An asymptotic analysis reveals that all the terms are bounded as $\xi \to 0$, but as $\xi \to \infty$ the first term of the first kernel is divergent. This is corrected by adding and subtracting the term

$$\frac{h^3}{6}\int_0^c \phi(t)\int_0^\infty \cos(\xi x)J_1(\xi t)\,d\xi\,dt$$

in eqn (2.45) as follows:

$$-\frac{h^3}{6}\int_0^c \phi(t)\int_0^\infty \cos(\xi x)J_1(\xi t)\,d\xi\,dt + \int_0^c \phi(t)\int_0^\infty \left\{\frac{h^3}{6}\left(\frac{\beta + \operatorname{sh}\beta\operatorname{ch}\beta}{\beta^2 - \operatorname{sh}^2\beta} + 1\right)\cos(\xi x)\right.$$
$$+ \frac{h^3}{12(1-\nu)}\frac{\beta - (3-2\nu)\operatorname{sh}\beta}{\beta(\beta - \operatorname{sh}\beta)}\cos(\xi l_0) + \frac{l_0(l - l_0/2)}{\xi}\cos\xi(l - l_0)$$
$$\left. - \frac{l_0}{\xi^2}\sin\xi(l - l_0) - \frac{x^2}{2\xi}\cos\xi(l - l_0)\right\} J_1(\xi t)\,d\xi\,dt$$
$$+ \int_0^c \psi(t)\int_0^\infty \left\{\frac{h^3}{12(1-\nu)}\left(\frac{\beta - (3-2\nu)\operatorname{sh}\beta}{\beta(\beta - \operatorname{sh}\beta)}\right)\sin(\xi l_0) - \frac{l_0(l - l_0/2)}{\xi}\sin\xi(l - l_0)\right.$$
$$\left. - \frac{l_0}{\xi^2}\cos\xi(l - l_0) + \frac{x^2}{2\xi}\sin\xi(l - l_0)\right\} J_0(\xi t)\,d\xi\,dt = 0. \tag{2.46}$$

After simplification, eqn (2.46) becomes

$$\frac{h^3}{6}\phi(x) + \int_0^c \psi(t)K_3(x, t)\,dt - \int_0^c \phi(t)K_4(x, t)\,dt = 0, \tag{2.47}$$

where

$$K_3(x, t) = \frac{\pi}{4}x^2, \tag{2.48}$$

$$K_4(x, t) = \int_0^\infty \frac{h^3}{6}\left(\frac{\beta + \operatorname{sh}\beta\operatorname{ch}\beta}{\beta^2 - \operatorname{sh}^2\beta} + 1\right)\xi x J_1(\xi x)J_1(\xi t)\,d\xi. \tag{2.49}$$

Equations (2.42) and (2.47) are the two coupled integral equations for the unknown auxiliary functions $\psi(x)$, $\phi(x)$. These equations are solved numerically. Once $\psi(x)$, $\phi(x)$ are obtained, all necessary physical quantities may be calculated.

Stresses may be calculated using eqn (2.19):

$$\tau_{yy}(x, 0) = \int_x^c \frac{\psi(t)\,dt}{\sqrt{(t^2 - x^2)}} + x\int_x^c \frac{\phi(t)\,dt}{t\sqrt{(t^2 - x^2)}}. \tag{2.19}$$

The resultant load due to the symmetric stresses is obtained as follows:

$$P = -\int_{-c}^{c} \tau_{yy}\,dx = -\pi\int_0^c \psi(t)\,dt. \tag{2.50}$$

The resultant moment due to the antisymmetric stresses is obtained as follows:

$$M = -\int_{-c}^{c} x\tau_{yy}\,dx = -\frac{\pi}{2}\int_0^c t\phi(t)\,dt. \tag{2.51}$$

In order to evaluate the deflection under the indenter Δ, the constant a_0 must be determined. Superimposing eqns (2.15) and (2.24) yields

$$u_y(x, 0) = \frac{1-\nu}{\mu}\int_0^\infty \frac{\beta + \operatorname{sh}\beta\operatorname{ch}\beta}{\xi(\beta^2 - \operatorname{sh}^2\beta)}[E_S(\xi)\cos(\xi x)$$
$$+ E_A(\xi)\sin(\xi x)]\,d\xi + a_0 + a_1x + a_2x^2 + a_3x^3. \tag{2.52}$$

Applying eqn (2.7) yields

$$a_0 = -\left(\frac{1-\nu}{\mu}\right)\int_0^\infty \frac{\beta + \operatorname{sh}\beta \operatorname{ch}\beta}{\beta^2 - \operatorname{sh}^2\beta}\,[E_S(\xi)\cos(\xi l_0) - E_A(\xi)\sin(\xi l_0)]\,\frac{d\xi}{\xi} + a_1 l_0 - a_2 l_0^2 + a_3 l_0^3, \quad (2.53)$$

where a_1, a_2 and a_3 are given by eqns (2.33)–(2.35). Substituting eqns (2.33)–(2.35) and (2.53) into eqn (2.52), and recalling that $u_y(0, 0) = \Delta$, yields

$$\begin{aligned}\Delta = &\int_0^c \psi(t)\left[\int_0^\infty \left\{\frac{1-\nu}{\mu}\frac{\beta + \operatorname{sh}\beta\operatorname{ch}\beta}{\beta^2 - \operatorname{sh}^2\beta}\left(\frac{1-\cos\xi l_0}{\xi}\right) + \frac{l_0}{2\mu}\frac{\beta - (3-2\nu)\operatorname{sh}\beta}{\beta(\beta - \operatorname{sh}\beta)}\right.\right.\\ &\left.\left.\times \sin(\xi l_0) - \frac{l_0^2}{2D}\frac{\cos\xi(l-l_0)}{\xi^2}\right\} J_0(\xi t)\,d\xi - \frac{\pi}{12D} l_0^2(3l - l_0)\right] dt\\ &+ \int_0^c \phi(t)\left[\int_0^\infty \left\{\frac{1-\nu}{\mu}\frac{\beta + \operatorname{sh}\beta\operatorname{ch}\beta}{\beta^2 - \operatorname{sh}^2\beta}\frac{\sin\xi l_0}{\xi} + \frac{l_0}{2\mu}\frac{\beta - (3-2\nu)\operatorname{sh}\beta}{\beta(\beta - \operatorname{sh}\beta)}\right.\right.\\ &\left.\left.\times \cos(\xi l_0)\right\} J_1(\xi t)\,d\xi - \frac{\pi t}{8D} l_0^2\right] dt. \end{aligned} \quad (2.54)$$

An asymptotic analysis reveals that both kernels are bounded as $\xi \to 0$, but the first two terms in each kernel are divergent as $\xi \to \infty$. This is adjusted by adding and subtracting the appropriate terms to yield

$$\Delta = \int_0^c \psi(t) K_5(t)\,dt + \int_0^c \phi(t) K_6(t)\,dt, \quad (2.55)$$

where

$$\begin{aligned}K_5(t) = &\frac{1-\nu}{\mu}\int_0^\infty \left\{\left(\frac{\beta + \operatorname{sh}\beta\operatorname{ch}\beta}{\beta^2 - \operatorname{sh}\beta^2} + 1\right)\left(\frac{1-\cos\xi l_0}{\xi}\right) - \frac{l_0}{h}\frac{\sin(\xi l_0)}{\beta - \operatorname{sh}\beta}\right.\\ &\left. - \frac{3l_0^2}{h^3}\frac{\cos\xi(l-l_0)}{\xi^2}\right\} J_0(\xi t)\,d\xi - \frac{1-\nu}{\mu}\cosh^{-1}\left(\frac{l_0}{t}\right)\\ &+ \frac{\pi}{4}\frac{3-2\nu}{\mu h} l_0 - \frac{\pi}{12D} l_0^2(3l - l_0), \end{aligned} \quad (2.56)$$

$$\begin{aligned}K_6(t) = &\frac{1-\nu}{\mu}\int_0^\infty \left\{\left(\frac{\beta + \operatorname{sh}\beta\operatorname{ch}\beta}{\beta^2 - \operatorname{sh}^2\beta} + 1\right)\frac{\sin(\xi l_0)}{\xi} - \frac{l_0}{h}\frac{\cos(\xi l_0)}{\beta - \operatorname{sh}\beta}\right\} J_1(\xi t)\,d\xi\\ &- \frac{1-\nu}{\mu}\frac{t}{l_0 + \sqrt{(l_0^2 - t^2)}} - \frac{\pi t}{8D} l_0^2. \end{aligned} \quad (2.57)$$

A quantity of interest in this problem, as well as in the subsequent study of the dynamic case, is the rotation of the beam under the indenter. More specifically, the rotation of the beam at the point under the indenter about which the moment produced by the antisymmetric stresses is zero (i.e. the "eccentricity" of the load) is of special interest. This point is obtained from statics simply as

$$x = -e = M/P. \quad (2.58)$$

Superimposing eqns (2.23) and (2.29), and making use of eqns (2.17), (2.18) and (2.33)–(2.35), yields

$$\bar{\theta}(x) = \frac{1}{D}\int_0^c \psi(t)\int_0^\infty \left\{\frac{h^3}{12(1-\nu)}\frac{\beta - (3-2\nu)\,\mathrm{sh}\,\beta}{\beta(\beta - \mathrm{sh}\,\beta)}(\sin\xi x + \sin\xi l_0)\right.$$
$$\left. - [l_0(l - l_0/2) + x(l - l_0) - x^2/2]\frac{\sin\xi(l-l_0)}{\xi} - (l_0 + x)\frac{\cos\xi(l-l_0)}{\xi^2}\right\}$$
$$\times J_0(\xi t)\,\mathrm{d}\xi\,\mathrm{d}t + \frac{1}{D}\int_0^c \phi(t)\int_0^\infty \left\{-\frac{h^3}{12(1-\nu)}\frac{\beta - (3-2\nu)\,\mathrm{sh}\,\beta}{\beta(\beta - \mathrm{sh}\,\beta)}\right.$$
$$\times (\cos\xi x - \cos\xi l_0) + [l_0(l - l_0/2) + x(l - l_0) - x^2/2]\frac{\cos\xi(l-l_0)}{\xi}$$
$$\left. - (l_0 + x)\frac{\sin\xi(l-l_0)}{\xi^2}\right\} J_1(\xi t)\,\mathrm{d}\xi\,\mathrm{d}t. \tag{2.59}$$

Note that the boundary condition $\bar{\theta}(-l_0) = 0$ is automatically satisfied by eqn (2.59). An asymptotic analysis of the kernels in eqn (2.59) reveals that they are bounded as $\xi \to 0$, but that as $\xi \to \infty$, the first term in each is divergent. This can be adjusted as before to become the following:

$$\bar{\theta}(x) = \frac{1}{D}\int_0^c \psi(t)\left\{\int_0^\infty \left[-\frac{h^3}{6}\left(\frac{\sin\xi x + \sin\xi l_0}{\beta - \mathrm{sh}\,\beta}\right) - (x + l_0)\frac{\cos\xi(l-l_0)}{\xi^2}\right] J_0(\xi t)\,\mathrm{d}\xi\right.$$
$$\left. - \frac{\pi}{2}[l_0(l - l_0/2) + x(l - l_0) - x^2/2] + \frac{\pi h^2}{24}\frac{3-2\nu}{1-\nu}\right\}\mathrm{d}t$$
$$+ \frac{1}{D}\int_0^c \phi(t)\left\{\int_0^\infty \left[\frac{h^3}{6}\left(\frac{\cos\xi x - \cos\xi l_0}{\beta - \mathrm{sh}\,\beta}\right) J_1(\xi t)\right]\mathrm{d}\xi - \frac{\pi}{4}(l_0 + x)\right\}\mathrm{d}t$$
$$+ \mathrm{sgn}(x)\left(\frac{3-2\nu}{2\mu h}\right)\left[\frac{\pi}{2}\int_0^{|x|}\psi(t)\,\mathrm{d}t - \int_{|x|}^c \psi(t)\sin^{-1}\left(\frac{|x|}{t}\right)\mathrm{d}t\right] H(c - |x|)$$
$$- \frac{3-2\nu}{2\mu h}H(c - |x|)\int_{|x|}^c \frac{\phi(t)}{t}\sqrt{(t^2 - x^2)}\,\mathrm{d}t. \tag{2.60}$$

Thus we can easily evaluate $\bar{\theta}$ $(x = -e)$.

3. PROBLEM SOLUTION

In order to be able to solve for the auxiliary functions $\psi(x)$ and $\phi(x)$, eqns (2.42)–(2.44) and (2.47)–(2.49) must be nondimensionalized. This is accomplished by the use of the following nondimensional parameters:

$$\delta = c/h, \tag{3.1a}$$
$$\epsilon = e/h, \tag{3.1b}$$
$$\alpha = l_0/h, \tag{3.1c}$$
$$\gamma = l/h, \tag{3.1d}$$
$$u = t/c, \tag{3.1e}$$
$$y = x/c, \tag{3.1f}$$
$$\psi(x) = \frac{Dcy}{Rh^3}\Psi(y), \tag{3.2}$$
$$\phi(x) = \frac{Dcy}{Rh^3}\Phi(y). \tag{3.3}$$

Once the nondimensionalized auxiliary functions $\Psi(y)$, $\Phi(y)$ are obtained, eqns (2.19), (2.50), (2.51), (2.55)–(2.57) and (2.60) can be used to calculate nondimensionalized stresses, loads, moments, deflections and rotations, respectively. These nondimensional quantities may be transformed back to real quantities via the following relationships:

$$\tau_{yy} = P\,\hat{\tau}_{yy}/c, \tag{3.4}$$

$$P = h^2\mu\hat{P}/(1-\nu)R, \tag{3.5}$$

$$M = h^3\mu\hat{M}/(1-\nu)R, \tag{3.6}$$

$$\Delta = h^2\hat{\Delta}/R, \tag{3.7}$$

$$\bar{\theta} = h\,\hat{\bar{\theta}}/R. \tag{3.8}$$

In order to assess the accuracy of the results for displacement and rotation under the indenter, the following beam-theory solutions are used:

$$\Delta_B = \frac{1}{3D}Pl_0^3 + \frac{1}{2D}Ml_0^2, \tag{3.9}$$

$$\bar{\theta}_B = \frac{1}{2D}P(l_0^2 - e^2) + \frac{1}{D}M(l_0 - e). \tag{3.10}$$

It should be noted that, although the formulation of the equations in this paper is such that they can be adapted to plane stress or plane strain, the use of beam-theory equations in comparison studies dictates that conditions of plane stress should be assumed in the evaluation of eqns (2.55) and (2.60). This assumption would be consistent with the use of a thin beam in an experimental verification of the results presented here. For the numerical evaluation of eqns (2.55) and (2.60), under conditions of plane stress, Poisson's ratio is taken to be equal to 0.35 [this corresponds to a Poisson's ratio of 0.26, if eqns (2.55) and (2.60) were to be evaluated under conditions of plane strain].

4. OBSERVATIONS AND CONCLUSIONS

Solutions to the problem were obtained for $\delta = 0.2$, 0.5 and 1.0, $\gamma = 5.0$, 10.0, 15.0 and 20.0, and for each γ, $\alpha = 0.25\gamma$, 0.5γ, 0.75γ. It was found that the stress distributions for the different values of l/h remained virtually identical. This is illustrated in Tables 1 and 2, which compare peak symmetric and total stresses for different values of c/h and l_0/h. A typical symmetric stress distribution is shown in Fig. 2; that of the total stress under the indenter is shown in Fig. 3. As can be seen in Fig. 2, for small values of c/h, the Hertzian distribution approximates the stress under the indenter quite well. As c/h increases, the distribution changes significantly. In Fig. 3 we see that as c/h increases, the location of peak stress shifts to the left and the distribution becomes less and less parabolic. This is because, for small values of c/h, the indenter acts like a point load. Hence, for small c/h, we have a small region of concentrated stress.

Table 1. Maximum symmetric stresses (case I).

	$l/h=10.0$			$l/h=20.0$		
c/h	$l_0/h=2.5$	$l_0/h=5.0$	$l_0/h=7.5$	$l_0/h=5.0$	$l_0/h=10.0$	$l_0/h=15.0$
0.2	0.635	0.635	0.635	0.635	0.635	0.635
0.5	0.622	0.622	0.617	0.625	0.621	0.622
1.0	0.560	0.561	0.561	0.560	0.564	0.562

Table 2. Maximum total stresses (case I).

	$\ell/h=10.0$			$\ell/h=20.0$		
c/h	$\ell_0/h=2.5$	$\ell_0/h=5.0$	$\ell_0/h=7.5$	$\ell_0/h=5.0$	$\ell_0/h=10.0$	$\ell_0/h=15.0$
0.2	0.636	0.636	0.636	0.636	0.636	0.636
0.5	0.648	0.649	0.645	0.650	0.649	0.649
1.0	0.982	0.983	0.981	0.982	0.988	0.983

However, as c/h increases, the shape of the indenter becomes more and more significant. As such, the curvature of the beam is much more pronounced, and the location of peak stress shifts to the left of the origin.

Tables 3 and 4 show a comparison between the elasticity solution developed here and the classical beam-theory solution. The elasticity solution is seen to agree well with the beam-theory solution. However, as c/h approaches l_0/h, the two solutions differ to a much larger extent. This behavior is due to the fact that the elasticity solution is valid only for $c/h \ll l_0/h$.

It is important to note that the rotations in Table 4 have no meaning unless they

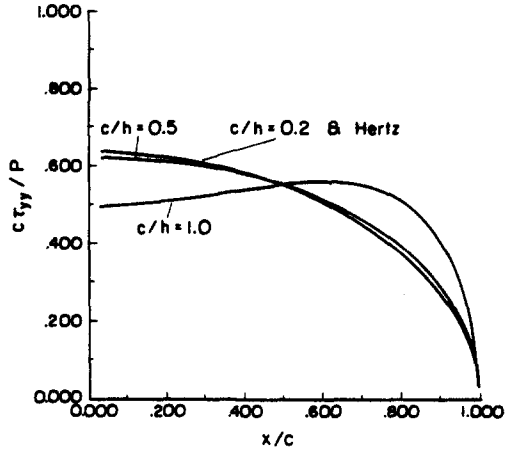

Fig. 2. Symmetric stress under the indenter (case I).

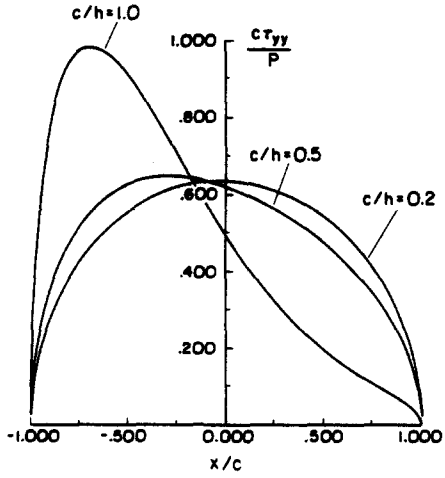

Fig. 3. Total stress under the indenter (case I).

Table 3. Displacement comparison (case I).

$\ell/h = 10.0$	$\ell_0/h=2.5$		$\ell_0/h=5.0$		$\ell_0/h=7.5$		
	Elasticity	Beam Theory	Elasticity	Beam Theory	Elasticity	Beam Theory	c/h
	2.0	2.0	16.1	16.1	54.3	54.3	0.2
	15.5	15.3	127.3	127.5	438.6	439.0	0.5
	376.2	383.5	3487.0	3498.0	8705.0	8716.0	1.0
$\ell/h = 20.0$	$\ell_0/h=5.0$		$\ell_0/h=10.0$		$\ell_0/h=15.0$		
	Elasticity	Beam Theory	Elasticity	Beam Theory	Elasticity	Beam Theory	c/h
	16.2	16.2	127.1	127.6	435.7	435.7	0.2
	128.5	128.8	1000.0	1001.0	3466.0	3467.0	0.5
	3327.0	3338.0	35890.0	35900.0	101540.0	101570.0	1.0

are converted to real values. Since the elasticity and beam-theory solutions were derived using small-angle approximations, it must be ensured that $\bar{\theta} < \bar{\theta}_0$, where $\bar{\theta}_0$ is a predetermined angle below which rotations are considered "small." Thus it is possible to place a lower bound on R, the radius of curvature of the indenter:

$$R/h > \hat{\theta}/\bar{\theta}_0. \tag{4.1}$$

However, it must also be ensured that no yielding occurs anywhere in the beam, i.e. that $\sigma_{max} < \sigma_y$, where

$$\sigma_{max} = M_{max}h/2I_0, \tag{4.2}$$

$$I_0 = h^3/12, \tag{4.3}$$

and σ_y is the yield stress of the material. The maximum moment occurs at the fixed end of the beam, and is given by

$$M_{max} = Pl_0 - M. \tag{4.4}$$

This condition on σ_{max} yields another lower bound on R:

$$R/h > 6\mu(\alpha\hat{P} - \hat{M})/(1 - \nu)\sigma_y. \tag{4.5}$$

Table 4. Rotation comparison (case I).

$\ell/h = 10.0$	$\ell_0/h=2.5$		$\ell_0/h=5.0$		$\ell_0/h=7.5$		
	Elasticity	Beam Theory	Elasticity	Beam Theory	Elasticity	Beam Theory	c/h
	1.1	1.2	4.8	4.8	10.8	10.9	0.2
	8.8	9.3	37.6	38.1	87.0	87.6	0.5
	186.4	215.9	985.8	1015.0	1683.0	1704.0	1.0
$\ell/h = 20.0$	$\ell_0/h=5.0$		$\ell_0/h=10.0$		$\ell_0/h=15.0$		
	Elasticity	Beam Theory	Elasticity	Beam Theory	Elasticity	Beam Theory	c/h
	4.8	4.9	19.0	19.1	43.5	43.6	0.2
	37.9	38.5	149.3	149.9	345.8	346.3	0.5
	940.5	969.0	5262.0	5269.0	10010.0	10040.0	1.0

Table 5. Minimum allowable values of R/h (case I).

	$l/h=10.0$			$l/h=20.0$		
c/h	$l_0/h=2.5$	$l_0/h=5.0$	$l_0/h=7.5$	$l_0/h=5.0$	$l_0/h=10.0$	$l_0/h=15.0$
0.2	4.0	14.0	31.0	14.0	55.0	125.0
0.5	26.0	108.0	250.0	109.0	428.0	991.0
1.0	535.0	2825.0	4824.0	2695.0	15080.0	28690.0

If $\bar{\theta}_0 = 20°$ (0.349 rad), $\sigma_y = 55{,}000$ ksi and $\mu = 11{,}510$ ksi, then eqns (4.1) and (4.5) may be combined into the following:

$$R/h > \max\{2.865\hat{\bar{\theta}},\ 1.696(\alpha\hat{P} - \hat{M})\}. \tag{4.6}$$

Judging from the values of $\hat{\bar{\theta}}$, $\hat{P}$ and $\hat{M}$, it is evident that $2.865\hat{\bar{\theta}} \gg 1.696(\alpha\hat{P} - \hat{M})$ for each case considered. Thus eqn (4.6) reduces to

$$R/h > 2.865\hat{\bar{\theta}}. \tag{4.7}$$

Under these criteria, Table 5 shows the minimum allowable values of R/h to ensure small deflections and no yielding. It is seen that for large c/h, and for long beams with $c/h > 0.5$, the indenter is practically flat. It is, therefore, of some interest to solve the problem of a flat indenter. This solution is found in the next section.

5. CASE II: FLAT INDENTER—PROBLEM FORMULATION

The problem to be solved is that of an elastic layer of thickness h and length l, indented by a flat punch on its upper surface [Fig. 1(b)]. The boundary conditions for the elasticity problem and beam-theory problem, whose solutions shall be superposed to form the solution to the actual problem, are as follows:

$$\tau_{yy}(x, h) = 0, \qquad |x| < \infty, \tag{5.1}$$

$$\tau_{xy}(x, h) = 0, \qquad |x| < \infty, \tag{5.2}$$

$$\tau_{xy}(x, 0) = 0, \qquad |x| < \infty, \tag{5.3}$$

$$\tau_{yy}(x, 0) = 0, \qquad c < |x| < \infty, \tag{5.4}$$

$$u_y(x, 0) = \Delta, \qquad 0 < |x| < c, \tag{5.5}$$

$$\bar{\theta} = 0, \qquad x = -l_0, \tag{5.6}$$

$$u_y = 0, \qquad x = -l_0, \tag{5.7}$$

$$M = 0, \qquad x = l - l_0, \tag{5.8}$$

$$V = 0, \qquad x = l - l_0. \tag{5.9}$$

It is further imposed that the stresses be nonsingular at $x = c$:

$$|\tau_{yy}(c, 0)| < \infty. \tag{5.10}$$

This condition ensures a smooth deflection of the beam for $x > 0$ and results in a "receding contact"[6]; here, as the load increases, the contact length *decreases* with load.

The suitable elasticity solution for this problem is given by eqns (2.11)–(2.15). Using this formulation, the normal stress is given by

$$\tau_{yy}(x, 0) = \int_0^\infty [E_S(\xi) \cos \xi x + E_A(\xi) \sin \xi x] \, d\xi. \tag{5.11}$$

For a flat punch, to have singularities at $x = \pm c$, we let

$$E_S(\xi) = AJ_0(\xi c) + \int_0^c \psi(t) J_0(\xi t) \, d\xi \tag{5.12}$$

$$E_A(\xi) = BJ_1(\xi c) + \int_0^c \phi(t) J_1(\xi t) \, d\xi. \tag{5.13}$$

Substituting into eqn (5.11) yields

$$\tau_{yy}(x, 0) = \frac{A + \frac{x}{c} B}{\sqrt{(c^2 - x^2)}} H(c - x) + \int_x^c \frac{\psi(t) \, dt}{\sqrt{(t^2 - x^2)}} + x \int_x^c \frac{\phi(t) \, dt}{t\sqrt{(t^2 - x^2)}}. \tag{5.14}$$

The first term in eqn (5.14) is singular at $x = \pm c$. For the singularity to vanish at $x = c$, it must be true that $A + B = 0$. Then eqn (5.14) becomes

$$\tau_{yy}(x, 0) = -\frac{B}{c} \frac{c - x}{\sqrt{(c^2 - x^2)}} H(c - x) + \int_x^c \frac{\psi(t) \, dt}{\sqrt{(t^2 - x^2)}} + x \int_x^c \frac{\phi(t) \, dt}{t\sqrt{(t^2 - x^2)}}. \tag{5.15}$$

The moment, shear and average slope are given by eqns (2.20), (2.21) and (2.23), respectively. As before, the beam-theory solution is taken to be

$$u_y^B(x) = a_0 + a_1 x + a_2 x^2 + a_3 x^3, \tag{5.16}$$

resulting in expressions for moment, shear and average slope given by eqns (2.27), (2.28) and (2.29), respectively. The constants a_1, a_2, a_3 are solved for as before with identical outcome. Equation (5.5) is treated in a similar manner. Differentiating with respect to x, and separating into symmetric and antisymmetric components, yields

$$\frac{\partial u_y^E}{\partial x}(x, 0)\bigg|_A + 2a_2 x = 0, \tag{5.17}$$

$$\frac{\partial u_y^E}{\partial x}(x, 0)\bigg|_S + a_1 + 3a_3 x^2 = 0. \tag{5.18}$$

Considering each equation one at a time, and following the same procedure as before, results in the following equations for A, B, $\psi(t)$ and $\phi(t)$:

$$AK_1(x, c) - \frac{h^3}{6} \psi(x) + \int_0^c \psi(t) K_1(x, t) \, dt + BK_2(x, c) + \int_0^c \phi(t) K_2(x, t) \, dt = 0, \tag{5.19}$$

$$AK_3(x, c) + \int_0^c \psi(t) K_3(x, t) \, dt - BK_4(x, c) + \frac{h^3}{6} \phi(x) - \int_0^c \phi(t) K_4(x, t) \, dt = 0, \tag{5.20}$$

where

$$K_1(x, \eta) = \int_0^\infty \left\{ \frac{h^3}{6} \left(\frac{\beta + \operatorname{sh}\beta \operatorname{ch}\beta}{\beta^2 - \operatorname{sh}^2\beta} + 1 \right) \xi x J_0(\xi x) + \frac{x}{\xi^2} \cos \xi(l - l_0) \right\} J_0(\xi\eta)\, d\xi + \frac{\pi}{2} x(l - l_0), \tag{5.21}$$

$$K_2(x, \eta) = \frac{\pi}{4} \eta x, \tag{5.22}$$

$$K_3(x, \eta) = \frac{\pi}{4} x^2, \tag{5.23}$$

$$K_4(x, \eta) = \int_0^\infty \frac{h^3}{6} \left(\frac{\beta + \operatorname{sh}\beta \operatorname{ch}\beta}{\beta^2 - \operatorname{sh}^2\beta} + 1 \right) \xi x J_1(\xi x) J_1(\xi\eta)\, d\xi \tag{5.24}$$

and $\eta = c$ or t. Equations (5.19) and (5.20) are two equations in four unknowns. A third equation was obtained earlier by enforcing nonsingularity of normal stress at $x = c$:

$$A + B = 0. \tag{5.25}$$

The fourth is found by enforcing the boundary condition given by eqn (5.5). After solving for the constant a_0 as before (with identical results), eqns (5.5), (2.15), (2.24), (5.12), (5.13) and (5.25) may be used in a manner analogous to that of solving for the displacement under the cylindrical indenter to solve for the constant B:

$$B = \frac{\Delta - \int_0^c \psi(t) K_5(t)\, dt - \int_0^c \phi(t) K_6(t)\, dt}{K_6(c) - K_5(c)}, \tag{5.26}$$

where

$$K_5(\eta) = \frac{1 - \nu}{\mu} \int_0^\infty \left\{ \left(\frac{\beta + \operatorname{sh}\beta \operatorname{ch}\beta}{\beta^2 - \operatorname{sh}^2\beta} + 1 \right) \left(\frac{1 - \cos \xi l_0}{\xi} \right) - l_0 \frac{\sin \xi l_0}{\beta - \operatorname{sh}\beta} \cdot - \frac{3 l_0^2 \cos \xi(l - l_0)}{h^3} \frac{}{\xi^2} \right\} J_0(\xi\eta)\, d\xi - \frac{1 - \nu}{\mu} \cosh^{-1}\left(\frac{l_0}{\eta} \right) + \frac{\pi}{4} \frac{3 - 2\nu}{\mu h} l_0 - \frac{\pi}{12D} l_0^2 (3l - l_0), \tag{5.27}$$

$$K_6(\eta) = \frac{1 - \nu}{\mu} \int_0^\infty \left\{ \left(\frac{\beta + \operatorname{sh}\beta \operatorname{ch}\beta}{\beta^2 - \operatorname{sh}^2\beta} + 1 \right) \frac{\sin \xi l_0}{\xi} - l_0 \frac{\cos \xi l_0}{\beta - \operatorname{sh}\beta} \right\} \times J_1(\xi\eta)\, d\xi - \frac{1 - \nu}{\mu} \frac{\eta}{l_0 + \sqrt{(l_0^2 - \eta^2)}} - \frac{\pi\eta}{8D} l_0^2, \tag{5.28}$$

and $\eta = c$ or t. Making use of eqns (5.25) and (5.26) in eqns (5.19) and (5.20) yields

$$\frac{h^3}{6} \psi(x) - \int_0^c \psi(t) \left\{ K_1(x, t) + \frac{K_1(x, c) - K_2(x, c)}{K_6(c) - K_5(c)} K_5(t) \right\} dt - \int_0^c \phi(t) \left\{ K_2(x, t) + \frac{K_1(x, c) - K_2(x, c)}{K_6(c) - K_5(c)} K_6(t) \right\} dt = \Delta \frac{-K_1(x, c) + K_2(x, c)}{K_6(c) - K_5(c)}, \tag{5.29}$$

$$\frac{h^3}{6}\phi(x) + \int_0^c \psi(t)\left\{K_3(x,t) + \frac{K_3(x,c) + K_4(x,c)}{K_6(c) - K_5(c)} K_5(t)\right\} dt - \int_0^c \phi(t)\left\{K_4(x,t) - \frac{K_3(x,c) + K_4(x,c)}{K_6(c) - K_5(c)} K_6(t)\right\} dt = \Delta \frac{K_3(x,c) + K_4(x,c)}{K_6(c) - K_5(c)}. \tag{5.30}$$

Thus eqns (5.29) and (5.30) are those used to solve for the unknown auxiliary functions $\psi(x)$, $\phi(x)$. These equations are solved numerically. Once $\psi(x)$, $\phi(x)$ are obtained, all necessary physical quantities may then be calculated.

Stresses may be calculated using eqn (5.15):

$$\tau_{yy}(x,0) = -\frac{B}{c}\frac{c-x}{\sqrt{(c^2-x^2)}} H(c-x) + \int_x^c \frac{\phi(t)\,dt}{\sqrt{(t^2-x^2)}} + x\int_x^c \frac{\phi(t)\,dt}{t\sqrt{(t^2-x^2)}} \tag{5.15}$$

where B is given by eqn (5.26). The resultant load due to the symmetric stresses is found to be given by

$$P = \pi B - \pi \int_0^c \psi(t)\,dt. \tag{5.31}$$

The resultant moment due to the antisymmetric stresses is found to be given by

$$M = -\frac{\pi}{2} cB - \frac{\pi}{2}\int_0^c t\phi(t)\,dt. \tag{5.32}$$

The rotation of the beam at any point $x > c$ is found to be given by

$$\bar{\theta}(x) = B[K_8(x,c) - K_7(x,c)] - B\frac{\pi}{4}\frac{3-2\nu}{\mu h} + \int_0^c \psi(t)K_7(x,t)\,dt + \int_0^c \phi(t)K_8(x,t)\,dt, \tag{5.33}$$

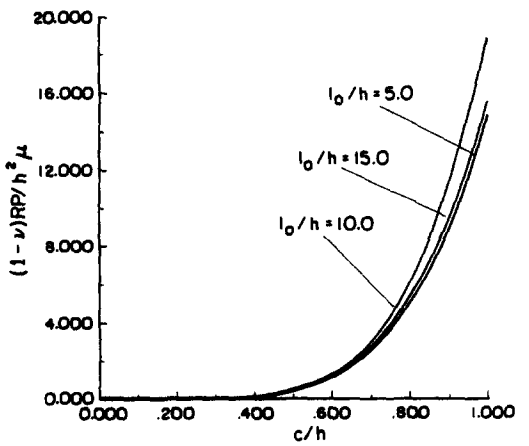

Fig. 4. Load-contact width (case I), $l/h = 20.0$.

where

$$K_7(x, \eta) = \frac{1}{D}\int_0^\infty \left[-\frac{h^3}{6}\left(\frac{\sin \xi x + \sin \xi l_0}{\beta - \operatorname{sh} \beta}\right) - (x + l_0)\frac{\cos \xi(l - l_0)}{\xi^2}\right] J_0(\xi\eta)\, d\xi$$
$$- \frac{\pi}{2D}[l_0(l - l_0/2) + x(l - l_0) - x^2/2] + \frac{\pi}{4}\frac{3 - 2\nu}{\mu h}, \quad (5.34)$$

$$K_8(x, \eta) = \frac{1}{D}\int_0^\infty \frac{h^3}{6}\left(\frac{\cos \xi x - \cos \xi l_0}{\beta - \operatorname{sh} \beta}\right) J_1(\xi\eta)\, d\xi - \frac{\pi}{4D}(l_0 + x)\eta, \quad (5.35)$$

and $\eta = c$ or t.

6. PROBLEM SOLUTION

Following a scheme similar to that of Section 3, we define

$$\alpha_1 = l_1/h, \quad (6.1)$$

$$\psi(x) = \frac{D\Delta cy}{h^5}\Psi(y), \quad (6.2)$$

$$\phi(x) = \frac{D\Delta cy}{h^5}\Phi(y). \quad (6.3)$$

Nondimensionalized stresses, loads, moments and rotations are calculated and may be transformed back to real quantities through

$$\tau_{yy} = P\hat{\tau}_{yy}/c, \quad (6.4)$$

$$P = \mu\Delta\hat{P}/(1 - \nu), \quad (6.5)$$

$$M = \mu\Delta\hat{M}/(1 - \nu), \quad (6.6)$$

$$\bar{\theta} = \Delta\hat{\theta}/h. \quad (6.7)$$

In order to assess the accuracy of the solution obtained, two tests are performed. First, the rotation of the beam just beyond $x = c$ is compared to that given by a standard beam-theory solution:

$$\bar{\theta}_B(\epsilon) = \frac{1}{2D}P(l_0^2 - \epsilon^2) + \frac{1}{D}M(l_0 + \epsilon), \quad (6.8)$$

where $\epsilon = c^+$. Second, from the nature of a receding contact problem, as the contact length decreases to zero, the load P_E increases to a certain limit value. Because the moment M_E goes to zero as the contact length goes to zero, the beam-theory solution for displacement tells us that the load P_E must approach the beam-theory load P_{BT} for a cantilever beam problem:

$$P_{BT} = 3D\Delta/l_0^3. \quad (6.9)$$

The limit load $\lim_{c/h\to 0}\hat{P}_E$ is compared to the value of $\hat{P}_{BT}$ for each case considered.

Once again, the use of beam-theory equations in subsequent comparison studies dictates that conditions of plane stress should be assumed in the solution of eqns (5.29) and (5.30). As before, Poisson's ratio is taken to be equal to 0.35 for the numerical solution of these equations.

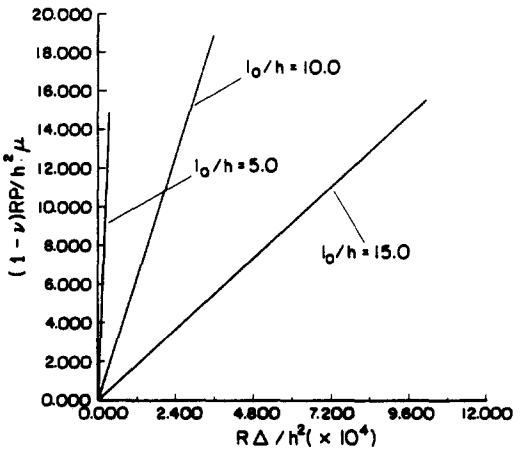

Fig. 5. Load-displacement (case I), $l/h = 20.0$.

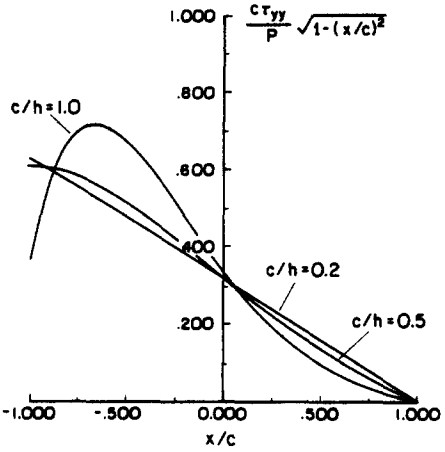

Fig. 6. Total stress under the indenter (case II).

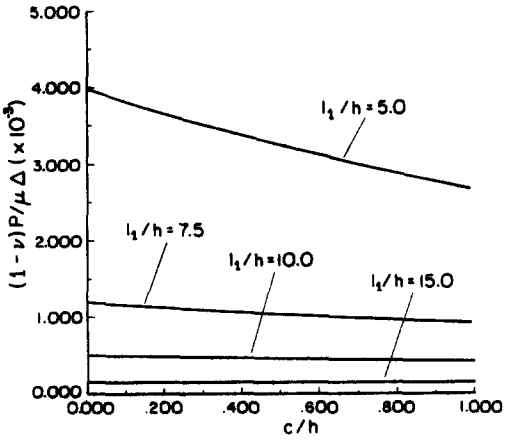

Fig. 7. Load-contact width (case II), $l/h = 20.0$.

Table 6. Rotation comparison (case II).

$\ell/h = 10.0$	$\ell_1/h=2.5$		$\ell_1/h=5.0$		$\ell_1/h=7.5$		
	Elasticity	Beam Theory	Elasticity	Beam Theory	Elasticity	Beam Theory	c/h
	0.508	0.544	0.280	0.285	0.192	0.193	0.2
	0.457	0.463	0.263	0.264	0.183	0.183	0.5
	0.403	0.303	0.239	0.219	0.172	0.166	1.0
$\ell/h = 20.0$	$\ell_1/h=5.0$		$\ell_1/h=10.0$		$\ell_1/h=15.0$		
	Elasticity	Beam Theory	Elasticity	Beam Theory	Elasticity	Beam Theory	c/h
	0.280	0.286	0.145	0.146	0.098	0.098	0.2
	0.263	0.264	0.140	0.140	0.095	0.095	0.5
	0.239	0.219	0.133	0.130	0.092	0.091	1.0

7. OBSERVATIONS AND CONCLUSIONS

Solutions to the problem were obtained for $\delta = 0.25$, 0.5 and 1.0, $\gamma = 10.0$ and 20.0, and for each γ, $\alpha_1 = 0.25\gamma$, 0.375γ, 0.5γ and 0.75γ. It was found that the stress distributions for the different values of l/h were virtually identical. A typical distribution of the total stress under the indenter, normalized by a factor of $\sqrt{(c^2 - x^2)}$, is shown in Fig. 6. An examination of the plots of the total stress under the indenter (Fig. 6), reveals that it is indeed singular at $x = -c$, but zero at $x = +c$. Furthermore, the stress distribution in Fig. 6 for $c/h = 1.0$ is seen to be an extreme case. This results from a more pronounced effect of the antisymmetric component in the solution for cases where c/h is large.

Tables 6 and 8 show a comparison between the solution developed here and the classical beam-theory solution. As can be seen, the elasticity solution agrees quite well with the beam-theory solution. Again it is noted that the rotations in Table 6 have no meaning unless they are converted to real values. Following the same procedure as before, an upper bound can be placed on the ratio of displacement under the indenter to beam thickness:

$$\Delta/h < \min\{\bar{\theta}_0/\hat{\theta}, (1 - \nu)\sigma_y/6\mu(\alpha\hat{P} - \hat{M})\}. \tag{7.1}$$

Assuming the same values of $\bar{\theta}_0$, σ_y and μ, eqn (7.1) reduces to

$$\Delta/h < 0.349/\hat{\theta}. \tag{7.2}$$

Under these criteria, Table 7 shows the maximum allowable values of Δ/h to ensure small rotations and no yielding.

Table 7. Maximum allowable values of Δ/h (case II).

	$\ell/h=10.0$			$\ell/h=20.0$		
c/h	$\ell_1/h=2.5$	$\ell_1/h=5.0$	$\ell_1/h=7.5$	$\ell_1/h=5.0$	$\ell_1/h=10.0$	$\ell_1/h=15.0$
0.2	0.68	1.24	1.81	1.24	2.39	3.54
0.5	0.76	1.32	1.90	1.32	2.48	3.63
1.0	0.86	1.46	2.02	1.46	2.62	3.82

Table 8. Limit load comparison (case II).

	ℓ_1/h	$\lim_{\delta \to 0} \hat{P}_E$ ($\times 10^{-2}$)	$\hat{P}_{BT}$ ($\times 10^{-2}$)
ℓ/h=10.0	2.5	3.104	3.200
	5.0	0.398	0.400
	7.5	0.118	0.119
ℓ/h=20.0	5.0	0.399	0.400
	10.0	0.049	0.050
	15.0	0.015	0.015

The phenomenon of receding contact in this problem is borne out by Fig. 7. As c/h goes to zero, the nondimensionalized load parameter approaches a limit value greater than zero. In Table 8, the limit load of the elasticity solution is seen to agree quite well with the limit load of the beam-theory solution. Furthermore, the limit load is highest in those cases where the indenter is close to the wall.

In Fig. 7 the relationships between the loads and contact widths for the various cases considered appear to violate the condition imposed on receding contact problems to ensure the existence and uniqueness of their solutions[6], since the contact lengths for a particular beam are not independent of the applied loads on that beam. The contact length in a receding contact problem will be independent of the level of loading, only if the ratio of the resultant moment to the applied load is constant for all levels of loading. In the problems solved through the course of this study, the ratio of moment to load changes as the applied loading changes; thus the contact length will change as well, the imposed conditions are not violated, and the problems studied are indeed receding contact problems.

Acknowledgement—The authors are grateful for support from the AFOSR (Grant AFOSR-82-0330).

REFERENCES

1. L. M. Keer and G. R. Miller, Smooth indentation of a finite layer. *ASCE J. Eng. Mech. Div.* **109**, 706–717 (1983).
2. L. M. Keer and R. Ballarini, Smooth contact between a rigid indenter and an initially stressed orthotropic beam. *AIAA J.* **21**, 1035–1042 (1983).
3. L. M. Keer and G. R. Miller, Contact between an elastically supported circular plate and a rigid indenter. *Int. J. Eng. Sci.* **21**, 681–690 (1983).
4. I. N. Sneddon, *Fourier Transforms*. McGraw-Hill, New York (1951).
5. G. N. Watson, *A Treatise on the Theory of Bessel Functions*, 2nd Edn. Cambridge University Press, Cambridge, Great Britain (1966).
6. J. Dundurs and M. Stippes, Role of elastic constants in certain contact problems. *J. Appl. Mech.* **37**, 965–970 (1970).